

Supporting Information

Thermal sprayed high-performance porous metal-supported solid oxide fuel cells with nanostructured $\text{La}_{0.6}\text{Sr}_{0.4}\text{Co}_{0.2}\text{Fe}_{0.8}\text{O}_{3-\delta}$ cathodes

Shan-Lin Zhang, Hai-Xin Yu, Cheng-Xin Li, Samson Yuxiu Lai, Chang-Jiu Li, Guan-Jun Yang, Hai-Bin Sun, Tao Wei, Meilin Liu*

Spray Parameters for LP-HVOF Flame Sprayed LSCF Cathodes

The LP-HVOF system (CH-2000) developed by Xi'an Jiaotong University was used for the LP-HVOF flame spraying process. Propane (C_3H_8) and oxygen (O_2) gases were applied to produce the supersonic flame. The liquid precursor solution was injected into the combustion chamber by a high pressure peristaltic pump (Qdos 30, Watson-Marlow, England). In order to get finer droplets, nitrogen (N_2) was added as the atomization gas by a specially designed injector.

Several spray parameters were varied to study their effects on cathode microstructure and performance, as summarized in **Table S1**. First, the cathodes were deposited at different spray distances (Case 1) in order to study the particles' heating and deposition behavior. The fuel and oxygen gas flow rates (Cases 2 through 4) were also varied to study the influence of the gas on the precursor's atomization, heating, and acceleration process. For these cases, the molar ratios of oxygen to fuel are similar (between 10 and 12).

Table S1. LP-HVOF spray parameters

| Parameter | Unit | Case-1 | Case-2 | Case-3 | Case-4 |
|--|----------------------|---------|--------|--------|--------|
| Pressure of fuel gas (C ₃ H ₈) | MPa | 0.4 | 0.4 | 0.4 | 0.4 |
| Pressure of oxygen gas (O ₂) | MPa | 0.65 | 0.65 | 0.65 | 0.65 |
| Flow rate of fuel gas (C ₃ H ₈) | slpm | 41 | 33 | 41 | 50 |
| Flow rate of oxygen gas (O ₂) | slpm | 330 | 330 | 500 | 590 |
| Pressure of atomization gas (N ₂) | MPa | 0.8 | 0.8 | 0.8 | 0.8 |
| Flow rate of atomization gas (N ₂) | slpm | 15 | 15 | 15 | 15 |
| Liquid precursor feed rate | ml min ⁻¹ | 40 | 40 | 40 | 40 |
| Deposition temperature | °C | <200 | <200 | <200 | <200 |
| Spray distance | mm | 40 – 80 | 40 | 40 | 40 |

Spray Parameters for PMS-SOFC's Fabrication

Table S2 shows the detailed spray parameters for the anode and electrolyte using APS and SAPS, respectively. An LSCF cathode with a thickness of 15 to 20 μm was deposited on the ScSZ electrolyte by LP-HVOF flame spray. The detailed spray parameters used were Case-4 from **Table S1**.

Table S2. Anode and electrolyte spray parameters.

| Parameter | Unit | Anode (APS) | Electrolyte (SAPS) |
|-----------------------------|---------------------|-------------|--------------------|
| Plasma arc power | kW | 36 | 72.5 |
| Arc voltage | V | 60 | 145 |
| Arc current | A | 600 | 500 |
| Flow rate of Ar | slpm | 50 | 70 |
| Flow rate of H ₂ | slpm | 4.5 | 26 |
| Powder feed rate | g min ⁻¹ | 25 | 25 |
| Deposition temperature | °C | <200 | 500–600 |
| Spray distance | mm | 100 | 100 |
| Thickness | μm | 20–30 | 30–35 |

Crystal Structure

Figure S1 shows the XRD patterns of as-sprayed LSCF cathodes deposited at different spray distances (**Figure S1a**) and for different cases (**Figure S1b**). Clearly, these XRD patterns are similar to the standard XRD pattern of La_{0.6}Sr_{0.4}Co_{0.8}Fe_{0.2}O₃ (PDF 48–0124), suggesting that single-phase, perovskite LSCF with a high degree of crystallization was found in all cases.

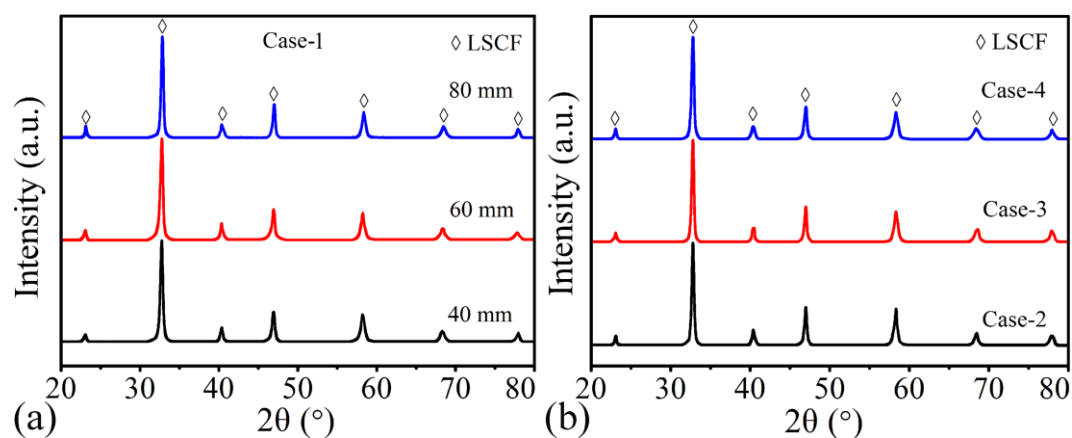


Figure S1. XRD patterns of LP-HVOF sprayed LSCF cathodes deposited at different spray parameters for a) Case-1 at different spray distances and b) in different cases.

Effect of Spray Distance on the Surface Morphologies of LP-HVOF Sprayed LSCF Cathodes

Figure S2 shows the surface morphologies of the LP-HVOF flame sprayed LSCF cathodes deposited at different spray distances. As shown in **Figure S2a**, the cathode deposited at 40 mm has a rough and porous island-like morphology. At higher magnification, (**Figure S2b**) it can be seen that the cathode was composed of agglomerates of spherical particles with a size of $\sim 0.1\text{--}0.5\ \mu\text{m}$. Moreover, the particles are well connected through sintering necks. As shown in **Figure S2c**, the big island-like features on the cathode surface disappeared when the spray distance was increased to 60 mm. At higher magnification, the microstructure (**Figure S2d**) indicates that the cathode was composed of spherical particles with a size of $\sim 0.5\text{--}1\ \mu\text{m}$ and some flattened spatters. The presence of spatters indicates that they were deposited while at least partially in a molten phase. The spherical particles were embedded in the deposit and bonded well with the melted parts. Also, microcracks were found on the cathode surface as indicated by the arrow. However, when the spray distance increased to 80 mm, the cathode had a smooth surface morphology and it was difficult to find any spherical particles (**Figure S2e**). The high magnification image (**Figure S2f**) suggests that almost all the cathode was deposited by molten droplets. Some microcracks still formed in the cathode during the spraying process as well.

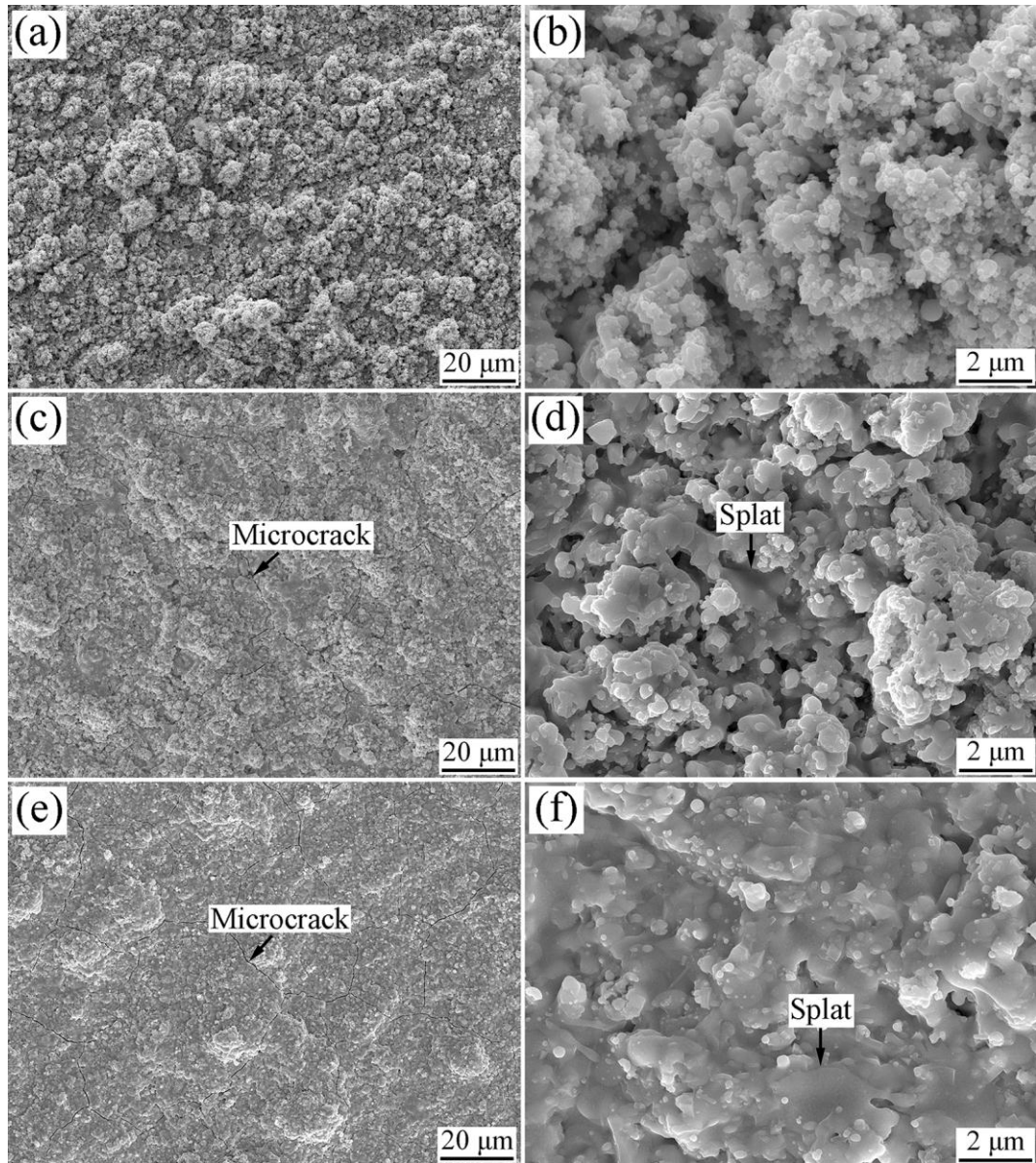


Figure S2. Surface morphologies of the LP-HVOF flame sprayed LSCF cathodes deposited at different spray distances (Case-1) of a) and b) 40 mm, c) and d) 60 mm, e) and f) 80 mm.

Effect of Gas Flow Rate on the Surface Morphologies of LP-HVOF Flame Sprayed LSCF Cathodes

Figure S3 shows the surface morphologies of the LSCF cathodes deposited in different cases. Similar to Case-1, the cathodes deposited in Case-2 (**Figure S4a**), Case-3 (**Figure S4c**) and Case-4 (**Figure S3e**) also showed a rough and porous island-like morphology. However, the size and surface roughness of the porous features decreased with the increase in fuel and

oxygen flow rates. A closer examination of the microstructure reveals that the cathodes were composed of small spherical particles, which were connected through sintering necks and a small amount of molten phase. Moreover, the particle size decreased with the increase in fuel and oxygen flow rates. In Case-2, the diameters of the particles ranged from $\sim 0.3\text{--}1\ \mu\text{m}$ and some flattened spatters were observed (**Figure S3b**). Under the conditions of Case-4, however, the particle size decreased to 50 to 200 nm (**Figure S3f**), producing a very fine nanostructure. With the increase of gas flow rate, the high flow rate of excess, unreacted oxygen gas has an increased cooling effect. Also, the gas velocity increased with the increase in gas flow rate, especially outside of the spray gun. Therefore, it can be concluded that the particles with a similar size can be heated to a lower temperature in Case-4 because of the lower flame temperature and higher acceleration process, and thus the grain growth rate of the fine particles could be further reduced during the flame spray process.

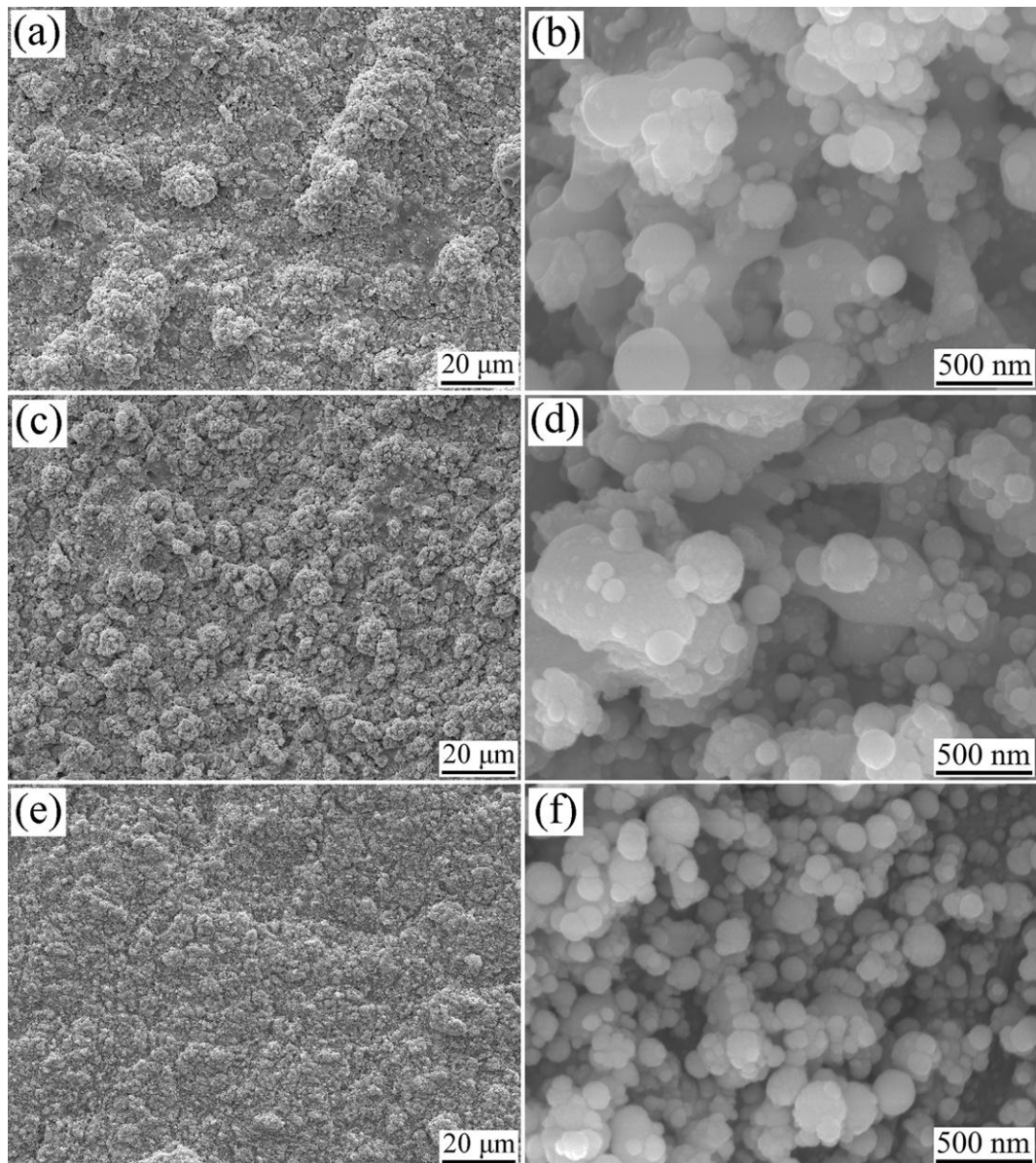


Figure S3. Surface morphologies of LP-HVOF flame sprayed LSCF cathodes deposited with different parameters in a) and b) Case-2; c) and d) Case-3; e) and f) Case-4.

Effect of spray parameters on the mean particle size

The mean particle sizes for the cathodes deposited in different cases are shown in **Figure S4**.

The mean particle size decreased rapidly with increasing gas flow rate, which is consistent with observations of the surface morphologies.

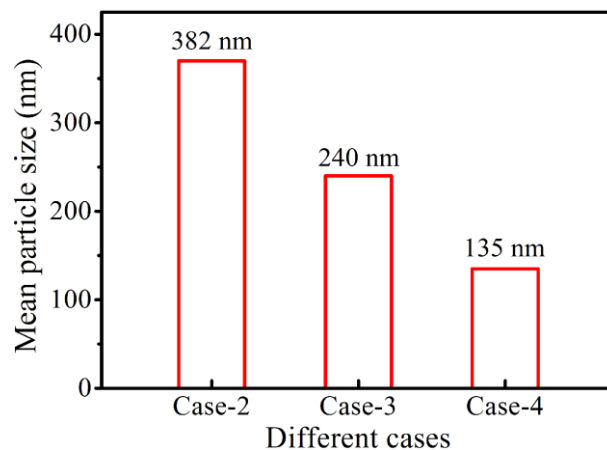


Figure S4. Mean particle sizes for the cathodes deposited in different cases of increasing gas flow rate.

Effect of Spray Parameters on the Electrochemical Performance

Figure S5a shows some typical impedance data for the symmetric cells assembled with LSCF cathodes deposited with different processing parameters. As expected, the cathode polarization resistances decreased when the gas flow rate was increased. For example, the polarization resistances measured at 600 °C were 1.2, 0.5, and 0.15 $\Omega \text{ cm}^2$ for the cathodes deposited under the conditions defined for Case-2, Case-3, and Case-4, respectively. When the measurement temperature was increased to 750 °C, the polarization resistances were 0.13, 0.07, and 0.025 $\Omega \text{ cm}^2$ for the cathodes deposited under the conditions defined for Case-2, Case-3, and Case-4, respectively. Compared to the Case-2 cathode, the polarization resistance for the Case-4 cathode decreased by 80.7%. The enhancement in cathode performance can also be attributed to the improvement in cathode microstructure. With the decrease in particle size, the TPBs for the ORR increased rapidly.

Figure S5b shows the temperature-dependent polarization resistance for the cathodes deposited under different processing conditions. The activation energy drops from 1.16 eV to 0.91 eV for LSCF cathodes when the fuel/oxygen gas flow rates increased from 33/340 slpm (Case-2) to 50/590 slpm (Case-4). With the increase in gas flow rates, the decrease in

activation energy can also be attributed to the decrease in particle or grain size. With the decrease in particle size, ionic conduction through grain boundaries is increased at lower temperatures and thus resulted in a higher oxygen diffusion rate. Therefore, the cathode showed a lower polarization resistance at lower temperatures and exhibited a lower activation energy. However, more research is needed to get an accurate analysis of the dominant mechanism for the cathode ORR.

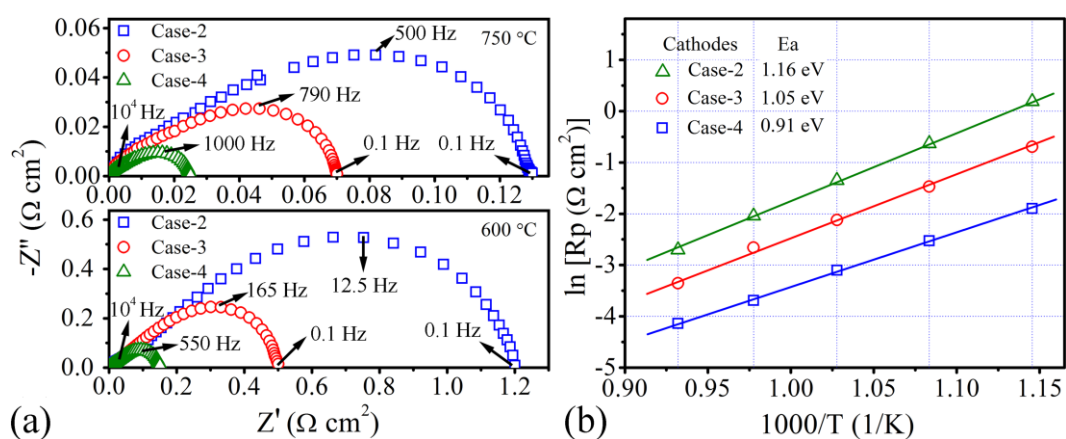


Figure S5. a) Electrochemical impedance spectra of LP-HVOF flame sprayed LSCF cathodes deposited in different cases, b) cathode polarization resistances for the LSCF cathodes deposited under different conditions.